Reinforcement-Learning-Based Cooperative Adaptive Cruise Control of Buses in the Lincoln Tunnel Corridor With Time-Varying Topology

Weinan Gao ^{ID}, *Member, IEEE*, Jingqin Gao ^{ID}, Kaan Ozbay, and Zhong-Ping Jiang ^{ID}, *Fellow, IEEE*

Abstract—The exclusive bus lane (XBL) is one of the most popular bus transit systems in the U.S. The Lincoln Tunnel utilizes an XBL through the tunnel in the AM peak period. This paper proposes a novel data-driven cooperative adaptive cruise control (CACC) algorithm that aims to minimize a cost function for connected and autonomous buses along the XBL. Different from existing model-based CACC algorithms, the proposed approach employs the idea of reinforcement learning, which does not rely on accurate knowledge of bus dynamics. Considering a time-varying topology, where each autonomous vehicle can only receive information from preceding vehicles that are within its communication range, a distributed controller is learned real-time by online headway, velocity, and acceleration data collected from the system trajectories. The convergence of the proposed algorithm and the stability of the closed-loop system are rigorously analyzed. The effectiveness of the proposed approach is demonstrated using a well-calibrated Paramics microscopic traffic simulation model of the XBL corridor. The simulation results show that the travel time in the autonomous version of the XBL are close to the present day travel time even when the bus volume is increased by 30%.

Index Terms—Reinforcement learning, connected and autonomous vehicles, cooperative adaptive cruise control, time-varying topology.

I. INTRODUCTION

THE Lincoln Tunnel is an 80-year-old, 1.5-mile-long tunnel that connects Weehawken, New Jersey and Manhattan, New York. It is one of the busiest crossings in the United States, carrying approximately 40 million vehicles in 2016 [1]. It also serves as one of the major bus transit corridors that directly connects to the Port Authority Bus Terminal (PABT) in midtown Manhattan, New York. The Lincoln Tunnel Exclusive Bus Lane, known as the XBL, is a 2.5-mile contra-flow bus lane traveling along New Jersey Route 495, leading from the New Jersey Turnpike to the Lincoln Tunnel [2]. The XBL acts as a one-lane isolated contraflow bus lane that operates only between 6-10AM every day and is separated from the oncoming traffic by cylindrical traffic delineators [3]. The XBL caters to an average of 1850 buses daily during peak hours (22% of peak-hour vehicles) and carries approximately 89% of peak-hour customers in the Lincoln Tunnel; see [2] and [4].

While the XBL is one of the most successful and productive bus rapid transit systems in the United States, the practical capacity of the XBL has often been exceeded during morning peak hours, resulting in considerable delays for the buses [5]. Fig. 1 shows an example of the congestion along the XBL. The Port Authority of New York and New Jersey (PANYNJ) predicts that the demand of daily buses using PABT will increase by 15% by 2040. This increasing demand urges the agencies to explore supply/demand strategies that can "increase or manage capacity along the Lincoln Tunnel Corridor - either by improving corridor operations or PABT facility operations [4]". A prior study completed in September 2016, entitled "Trans-Hudson Commuting Capacity Study", evaluates various strategies to meet the projected 2040 trans-Hudson commuter demand, taking into account the conceptual planning of PABT replacement [4]. This prior study suggests opportunities to develop new technologies, especially connected and automated vehicle technologies [6], to improve the operational efficiency of the Lincoln Tunnel corridor by dispatching in real time. The use of platooning buses via adaptive cruise control (ACC) or cooperative adaptive cruise control (CACC) technology could significantly increase the throughput of the existing XBL without any huge investment.

ACC is an enhancement of the classical cruise control algorithms that can reduce driver workload and fatigue. It automatically regulates the dynamics of individual vehicles by measuring the headway and velocity via on-board sensors, such as radars, lasers and video cameras. It is an example of application of real-time control techniques on traffic systems [7]–[9]. Ozbay *et al.* [10], [11] study the feasibility of automating the exclusive bus lane (XBL) in the Lincoln

Fig. 1.   Bus in the XBL (taken in June, 2017).

tunnel corridor using three different adaptive cruise controllers developed in Paramics simulation network, namely P controller, PI controller, and PID controller. These elementary linear controllers are achieved by adjusting the speed of the bus based on its speed and spacing measurements with respect to the bus ahead. The performance of each controller and the travel times are examined, and the results are compared with the simulation model that describes the traffic scenarios in 2005 with approximately 1,700 buses on the XBL during the peak period and a peak hour volume of 730 buses [3], [10]. The results have shown that all three controllers performed much better than the human driver in the simulation model. In addition, all the three controllers are able to stop the bus quickly and safely in the simulations in case of emergency. A qualitative cost analysis indicates that automation of the bus lane is beneficial.

CACC is an extended version of ACC. In comparison with the sensor-based ACC, the CACC technology has a longer communication range that enables it to alert drivers about potential collisions. This is more beneficial in some blind intersections. Additionally, CACC usually considers a longitudinal platoon of vehicles, and well-formed platoon with smaller time headway manipulated by CACC can further reduce aerodynamic drag, which leads to fuel saving.

In the last decade, several vehicular platoon control algorithms have been developed through model-based control theory. For instance, an optimal connected cruise control algorithm has been developed for a platoon of mixed human-driven and autonomous vehicles [12]. Considering the state and input constraints, the model predictive control (MPC) has been employed to design CACC algorithms for vehicular platoons [13], [14]. The robust MPC strategy has been utilized for CACC design in the presence of model uncertainties [15]. The effect of delay on the platoon performance has also been studied [12], [16], [17]. In our previous work [18], a data-driven adaptive optimal control approach has been proposed for a platoon of human-operated and autonomous vehicles in the presence of input delay.

The effectiveness of CACC on safety, traffic flow, and the environment has also been tested in different traffic scenarios with human-driven and autonomous vehicles [19]–[23]. Shladover *et al.* have compared the impact of CACC and ACC on freeway traffic flow [21]. They claim that ACC

marginally changes the lane capacity and that, while CACC can significantly improve the capacity. Moreover, the capacity increases as the penetration of autonomous vehicles increases. This is consistent with the conclusion drawn in [20]. van Arem *et al.* [20] study a freeway lane drop as a shockwave induced by a disturbance limits the traffic capacity. They disclose the fact that a high CACC-penetration rate ($>60\%$) can improve traffic flow while mitigating the serious shockwave effect, especially in the condition of high traffic volume. This is attributed to the increased average speed, dramatic reduction of the number of shock waves, and low speed variance. The influence of CACC on both traffic congestion and environment is investigated in [22]. Specifically, they explore the possibility of integrating both the CACC and intelligent traffic signals. The benefits of implementing the integrated algorithm are expected to reduce the traffic delay by up to 91% and reduce fuel consumption by up to 75%.

Although CACC has been extensively studied by many researchers, there are still some open issues when one implements this technology in connected buses on XBL. First, the existing CACC methods are usually model-based. The first step in the model-based control method is often building a mathematical model for the plant in question. However, system modeling often involves modeling errors. A controller designed based on an inaccurate model may destabilize the vehicle system, which threatens the safety of the autonomous buses and their surrounding traffic. Robust control can stabilize the vehicle system if there are errors or uncertainties in the model, but this compromises the system's transient response. Second, in order to ameliorate the transient performance and to reduce the fuel usage of the autonomous buses, one hopes to design an optimal controller through minimizing some predefined cost functions. Nevertheless, a common feature of most optimal control methods is that they rely on the accurate knowledge of the system model. Last but not least, in the framework of connected vehicles and CACC, each vehicle is supposed to receive information from preceding vehicles (active vehicles) who stay within the communication range. Notice that the number of active vehicles usually varies since the relative distances between buses change with time. This renders the communication topology as time-varying, which is usually a challenge for the adaptive/optimal control design.

In order to overcome these technical obstacles, this paper proposes a novel data-driven distributed control strategy for connected and autonomous buses on XBL. To be more specific, the proposed control strategy employs the idea of reinforcement learning (RL) [24]–[32]. RL is an active research branch of artificial intelligence, which is viewed as a practically sound data-driven optimal control approach as well. The main feature of RL is that it is able to approximate the optimal control strategy and the corresponding cost function in an iterative fashion, without accurate knowledge of the vehicle dynamics. This feature helps overcome two main drawbacks of the traditional dynamic programming, i.e., the curse of dimensionality [33] and curse of modeling [34].

The contributions of this paper are listed as follows.
1) A novel data-driven CACC method for connected and autonomous buses is proposed through RL. This is

different from most existing model-based CACC methods [12]–[14], [16], [17] in that the former essentially relies on the collected online headway, velocity, and acceleration data. The proposed RL algorithm can be used to learn the optimal controllers with a satisfactory transient response in the absence of prior knowledge of vehicle dynamics.

2) This paper distinguishes itself from our previous work [35], [36] through combining the ideas of RL and distributed control [37]. Compared with centralized control, distributed control strategies do not rely on the assumption that each vehicle can communicate with a central location and share information by a fully connected network, which reduces communication cost. Also, it is widely accepted that centralized control is fragile as it requires the information of all the agents in the network. In this sense, the distributed control strategy is more robust to communication failure or information loss, as it uses only the information of neighboring agents within the communication range.

3) To the best of our knowledge, the time-varying topology, or more accurately the state-dependent connectivity [38], is considered for the CACC design for the first time. The connectivity of vehicles depends on the relative distance and communication range, making this approach more reflective of real-world conditions. The data-driven controller design is constructive, while the closed-loop system stability and optimality analyses are rigorously completed in this scenario.

The remainder is organized as follows. In Section II, we develop a Paramics micro-traffic simulation model, which is calibrated by real traffic data. In Section III, the data-driven CACC is designed along with stability and optimality analyses. The traffic simulation results are included in Section IV. Concluding remarks and future work are contained in Section V.

Notations: Throughout this paper, $\mathbb{C}^-$ stands for the open left-half complex plane. $|\cdot|$ represents the Euclidean norm for vectors and the induced norm for matrices. $\otimes$ indicates the Kronecker product operator and $\text{vec}(A) = [a_1^T, a_2^T, \cdots, a_m^T]^T$, where $a_i \in \mathbb{R}^n$ are the columns of $A \in \mathbb{R}^{n \times m}$. For a symmetric matrix $P \in \mathbb{R}^{m \times m}$, $\text{vecs}(P) = [p_{11}, 2p_{12}, \cdots, 2p_{1m}, p_{22}, 2p_{23}, \cdots, 2p_{m-1,m}, p_{mm}]^T \in \mathbb{R}^{\frac{1}{2}m(m+1)}$. For an arbitrary column vector $v \in \mathbb{R}^m$, $|v|_P$ stands for $v^T P v$, and $\text{vecv}(v) = [v_1^2, v_1 v_2, \cdots, v_1 v_m, v_2^2, v_2 v_3, \cdots, v_{m-1} v_m, v_m^2]^T \in \mathbb{R}^{\frac{1}{2}m(m+1)}$. $\lambda_M(P)$ and $\lambda_m(P)$ denote the maximum and the minimum eigenvalue of a real symmetric matrix P, respectively.

II. MICROSCOPIC TRAFFIC SIMULATION MODEL OF XBL

Paramics is a micro-traffic simulation software that is widely used for the study of traffic operations. The software allows users to setup vehicles, traffic signals, ramps, and so forth. Fig. 2 shows the network simulation model that is built in Paramics. The Paramics model simulates the one-lane bus-only XBL from 6AM to 10AM. The one-lane structure restricts any

Fig. 2. Paramics model of the Lincoln Tunnel corridor [10].

merge, split or lane changing behaviors for buses. There are no interactions between buses and general traffic on the XBL.

First, we develop the skeleton network by placing nodes and connecting these nodes using links. Other stages include assigning priorities at junctions, defining vehicle types, setting restrictions and demands. After that, we calibrate the traffic network such that the simulation results match traffic data extracted from the Lincoln Tunnel. The Origin-Destination (O-D) matrices are estimated for 15-minute intervals based on the traffic volumes obtained from New Jersey Department of Transportation and New York City Department of Transportation, and the toll plaza demand data [39]. The current number of buses utilizing XBL is obtained from PANYNJ's official website with 1850 buses during peak period [2]. Taking advantage of buses equipped with GPS devices, the travel time and headway information of buses are extracted via New Jersey Transit (NJT) "MyBus Now" platform [40], a real-time service information system that provides estimated vehicle arrival times and map locations for NJT buses. A web scraper that behaves as a "virtual sensor" [41] is developed to retrieve real-time bus schedules and delays for the corresponding bus lines from "MyBus Now" [42]. More details about the virtual sensor methodology can be found in [41]. One month of bus data (Apr. to May, 2017) are processed and cleaned. The model is then calibrated by modifying certain features such as reaction times and safe headways so that it replicates the existing traffic conditions. Ten simulation runs are performed with different random seeds so that the stochasticity associated with the microsimulation model can be minimized. Geoffrey E. Heavers (GEH) statistic is used to compare the field bus volumes with simulation bus volumes. Ten simulation results with different random seeds show that 91% observed GEHs were less than 5. The difference between field travel times and model travel times remains less than 10% on all time intervals except two occasions when it increases to 11%−13%. Moreover, the mean of model travel time μ_M is selected to compare with the mean of field travel time μ_F with two-sample t-test. It shows that the hypothesis $\mu_M = \mu_F$ is accepted at 5% significant level. These results indicate that the calibrated network is consistent with that of the field traffic conditions. More information on issues related to large scale traffic calibration in general can be found in the previous

study [43]. Note that the travel times collected through NJT MyBus Now application are for buses traveling from the teardrop on the New Jersey side (entry point of XBL, refer to Fig. 2 to PABT at Manhattan. The same entering and exit points are used to collect travel time from the micro-simulation model.

III. CONTROLLER DESIGN

In this Section, we first present the formulation of the CACC problem. Then, we propose a novel data-driven distributed controller design algorithm. The stability and optimality of the closed-loop system are rigorously analyzed.

Consider a platoon of n autonomous buses. Let h_i be the headway of ith vehicle in the platoon, i.e., the bumper-to-bumper distance between the ith vehicle and the $(i-1)$th vehicle. Time headway [44] and constant spacing [45] are two main spacing policies in the CACC. This paper adopts the former policy since there are different speed limits in each snap of the road. The desired headway is chosen by $h_i^*(t) = \tau v_i(t) + h_0$, where τ is the time headway and h_0 is named the standstill headway. Define $\Delta h_i(t) = h_i(t) - h_i^*(t)$ and $\Delta v_i(t) = v_{i-1}(t) - v_i(t)$. By [46], the dynamics of the ith vehicle can be described by

$$\dot{x}_i(t) = A_i x_i(t) + B_i u_i(t) + D_i x_{i-1}(t) \tag{1}$$

where u_i represents the desired acceleration of vehicle i. For $j = i - 1, i$, $x_k = [\Delta h_k, \Delta v_k, a_k]^T$ includes the headway and velocity errors, and the acceleration of vehicle k. The system matrices are

$$A_i = \begin{bmatrix} 0 & 1 & -\tau \\ 0 & 0 & -1 \\ 0 & 0 & -\frac{1}{T_i} \end{bmatrix}, \quad B_i = \begin{bmatrix} 0 \\ 0 \\ \frac{G_i}{T_i} \end{bmatrix}, \quad D_i = \begin{bmatrix} 0 & 0 & 0 \\ 0 & 0 & 1 \\ 0 & 0 & 0 \end{bmatrix}$$

with G_i the system gain and T_i the system time constant.

Assume there is a fictitious vehicle running before the leading vehicle in a constant velocity. In this setting, the state x_1 of the leader in the platoon also satisfies the equation (1) with $x_0 \equiv 0$. Given the system (1), define a time-varying digraph $\mathcal{G}(t) = \{\mathcal{V}, \mathcal{E}(t)\}$. $\mathcal{V} = \{1, \cdots, n\}$ is the node set. $\mathcal{E}(t) \subset \mathcal{V} \times \mathcal{V}$ refers to the edge set. If the distance between vehicle i and k is smaller than the minimum between the communication range of vehicle k and i at time t, then the edge $(k, i) \in \mathcal{E}(t)$. Denote $\mathcal{N}_i(t)$ the set of all the nodes k such that $(k, i) \in \mathcal{E}(t)$. For instance, the set $\mathcal{N}_i(t) = \{i-1, i-2\}$ at time t since there are only two preceding vehicles staying in the communication range of vehicle i in Fig. 3. Interestingly, this time-varying topology depends on the system state, which is named state-dependent connectivity [38]. Moreover, the communication topology is unidirectional in this paper, which means each bus is only able to receive its preceding vehicle in the communication range.

One of control goals in this paper is to let the headway and velocity errors and acceleration of each bus asymptotically converge to zero, i.e., $\lim_{t \to \infty} x_i(t) = 0$ for $i = 1, 2, \cdots, n$. In order to improve the transient response of the system,
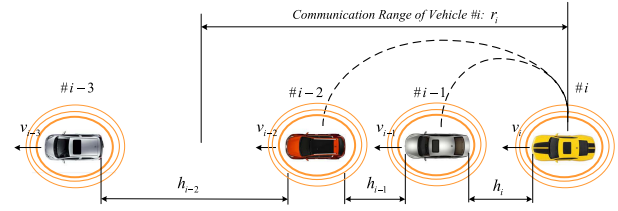

Fig. 3. Vehicle platoon with time-varying topology.

one can design an optimal controller through minimizing the following cost function

$$J = \int_0^\infty (x^T Q x + u^T R u) d\tau \tag{2}$$

where $Q = \text{blockdiag}(Q_1, Q_2, \cdots, Q_n)$, $R = \text{blockdiag}(R_1, R_2, \cdots, R_n)$, $x = [x_1^T, x_2^T, \cdots, x_n^T]^T$, and $u = [u_1, u_2, \cdots, u_n]^T$. By linear optimal control theory [47], there exists an optimal controller is $u = -Kx$ such that the cost function (2) achieves its minimum $J^* = x^T P^* x$. However, this optimal controller is centralized, which cannot be implemented in the vehicular platoon with state-dependent connectivity condition. Taking this scenario into consideration, if all the system matrices are available, then one can design the following model-based suboptimal distributed controller for each autonomous bus:

$$u_i(t) = -K_i^* \zeta_i(t) \tag{3}$$

where

$$\zeta_i(t) = \frac{1}{|\mathcal{N}_i(t)|} \sum_{k \in \mathcal{N}_i(t)} (x_i(t) - x_k(t)). \tag{4}$$

In (4), $|\mathcal{N}_i(t)|$ denotes the cardinality of the set $\mathcal{N}_i(t)$. If $\mathcal{N}_i(t) = \emptyset$, we split the platoon by letting vehicle i be a new leader operating in a constant speed. It is merged to the previous platoon until time T_i when $\mathcal{N}_i(T_i) \neq \emptyset$.

Choosing weight matrices such that $Q_i, R_i > 0$, the desired control gain for the ith vehicle can be computed by

$$K_i^* = R_i^{-1} B_i^T P_i^* \tag{5}$$

where matrix P_i^* indicates the solution to the following algebraic Riccati equation

$$A_i^T P_i^* + P_i^* A_i + Q_i - P_i^* B_i R_i^{-1} B_i^T P_i^* = 0. \tag{6}$$

However, the model-based control approaches (3) are hard to implement since identifying the system dynamics accurately is usually a challenging task. Also, it is almost impossible to know the system matrices of all the vehicles considering different types and conditions of vehicles on the road. We will propose a data-driven control approach to learn the distributed controller (3) without knowledge of system matrices A_i and B_i.

A. Data-Driven CACC Design

To begin with, we rewrite the system (1) as

$$\dot{x}_i = (A_i - B_i K_{ij}) x_i + B_i (K_{ij} x_i + u_i) + D_i x_{i-1} \tag{7}$$

where, for $j = 1, 2, \cdots$, the control gain K_{ij} is a stabilizing control gain.

Let P_{ij} be the unique solution to the following Lyapunov equation

$$(A_i - B_i K_{ij})^T P_{ij} + P_{ij}(A_i - B_i K_{ij}) + Q_i + K_{ij}^T R_i K_{ij} = 0, \tag{8}$$

and $K_{i,j+1}$ be updated by

$$K_{i,j+1} = R_i^{-1} B_i^T P_{i,j}. \tag{9}$$

Along the solutions to (7), by equations (8)-(9), it follows that

$$x_i^T(t + \delta t) P_{ij} x_i(t + \delta t) - x_i^T(t) P_{ij} x_i(t)$$
$$= \int_t^{t+\delta t} x_i^T[(A_i - B_i K_{ij})^T P_{ij} + P_{ij}(A_i - B_i K_{ij})] x_i d\tau$$
$$+ 2 \int_t^{t+\delta t} (u_i + K_{ij} x_i)^T B_i^T P_{ij} x_i d\tau$$
$$+ 2 \int_t^{t+\delta t} x_{i-1}^T D_i^T P_{ij} x_i d\tau$$
$$= - \int_t^{t+\delta t} x_i^T (Q_i + K_{ij}^T R_i K_{ij}) x_i d\tau$$
$$+ 2 \int_t^{t+\delta t} (u_i + K_{ij} x_i)^T R_i K_{i,j+1} x_i d\tau$$
$$+ 2 \int_t^{t+\delta t} x_{i-1}^T D_i^T P_{ij} x_i d\tau. \tag{10}$$

By Kronecker product representation, we obtain

$$x_i^T(Q_i + K_{ij}^T R_i K_{ij}) x_i = (x_i^T \otimes x_i^T) \text{vec}\left(Q_i + K_{ij}^T R_i K_{ij}\right),$$
$$x_{i-1}^T D_i^T P_{ij} x_i = (x_i^T \otimes x_{i-1}^T) \text{vec}\left(D_i^T P_{ij}\right),$$
$$(u_i + K_{ij} x_i)^T R_i K_{i,j+1} x_i = [(x_i^T \otimes x_i^T)(I \otimes K_{ij}^T R_i)$$
$$+ (x_i^T \otimes u_i^T)(I \otimes R_i)] \text{vec}\left(K_{i,j+1}\right).$$

Moreover, for any two vectors $a \in \mathbb{R}^{n_a}, b \in \mathbb{R}^{n_b}$ and a sufficiently large number $s > 0$, define

$$\delta_a = [\text{vecv}(a(t_1)) - \text{vecv}(a(t_0)), \cdots,$$
$$\text{vecv}(a(t_s)) - \text{vecv}(a(t_{s-1}))]^T \in \mathbb{R}^{s \times \frac{n_a(n_a+1)}{2}},$$
$$\Gamma_{a,b} = \left[\left[\int_{t_0}^{t_1} a \otimes b d\tau, \int_{t_1}^{t_2} a \otimes b d\tau, \cdots, \int_{t_{s-1}}^{t_s} a \otimes b d\tau\right]^T\right].$$
$$\in \mathbb{R}^{s \times n_a n_b}$$

(10) implies the following linear equation

$$\Psi_i^{(j)} \begin{bmatrix} \text{vecs}(P_{ij}) \\ \text{vec}(K_{i,j+1}) \\ \text{vec}\left(D_i^T P_{ij}\right) \end{bmatrix} = \Phi_i^{(j)} \tag{11}$$

where

$$\Psi_i^{(j)} = [\delta_{x_i}, -2\Gamma_{x_i x_i}(I \otimes K_{ij}^T R_i) - 2\Gamma_{x_i u_i}(I \otimes R_i),$$
$$- 2\Gamma_{x_i x_{i-1}}] \in \mathbb{R}^{s \times 18},$$
$$\Phi_i^{(j)} = -\Gamma_{x_i x_i} \text{vec}\left(Q_i + K_{ij}^T R_i K_{ij}\right) \in \mathbb{R}^s.$$

The full column rank of $\Psi_i^{(j)}$ is guaranteed under some mild conditions [48], [49] similar to persistent excitation, which

may be satisfied by adding some exploration noise into the control input. In this way, the solution to (11) can be uniquely obtained via

$$\begin{bmatrix} \text{vecs}(P_{ij}) \\ \text{vec}(K_{i,j+1}) \\ \text{vec}\left(D_i^T P_{ij}\right) \end{bmatrix} = \left[\left(\Psi_i^{(j)}\right)^T \Psi_i^{(j)}\right]^{-1} \left(\Psi_i^{(j)}\right)^T \Phi_i^{(j)} \tag{12}$$

Now, we are ready to propose our data-driven CACC algorithm, Algorithm 1 to approximate the control gain K_i^* in the distributed CACC (13).

Algorithm 1 Data-Driven CACC Algorithm
_____
1: $i \leftarrow 1$
2: **repeat**
3:     Apply an initial control policy $u_i = -K_{i0} x_i + e_i$ with exploration noise e_i and K_{i0} a stabilizing control gain.
4:     $j \leftarrow 0$
5:     **repeat**
6:         Solve P_{ij} and $K_{i,j+1}$ from (12) via online input-state data.
7:         $j \leftarrow j + 1$
8:     **until** $|P_{ij} - P_{i,j-1}| < \epsilon_i$ with ϵ_i a small positive constant.
9:     $j^* \leftarrow j$
10:    Obtain the following suboptimal controller

$$u_i^\dagger = -K_{i,j^*} \zeta_i \tag{13}$$

11:    $i \leftarrow i + 1$
12: **until** $i = n + 1$
_____

The convergence of the proposed Algorithm 1 is analyzed in the following.

Theorem 1: For $i = 1, 2, \cdots, n$, the sequences $\{P_{i,j}\}_{j=0}^\infty$ and $\{K_{i,j}\}_{j=1}^\infty$ computed through Algorithm 1 converge to P_i^* and K_i^*, respectively.

Proof: For all $i = 1, 2, \cdots, n$, it is checkable that matrices P_{ij} and K_{ij} that are uniquely determined by (12) solve equations (8)-(9). By [50], as the iteration $j \rightarrow \infty$, matrices P_{ij} and K_{ij} solving from (8)-(9) converge to matrices P_i^* and K_i^*, respectively. This immediately implies the convergence of sequences $\{P_{i,j}\}_{j=0}^\infty$ and $\{K_{i,j}\}_{j=1}^\infty$ determined by (12). The proof is thus completed. $\square$

Remark 1: Note that Algorithm 1 employs the idea from the policy iteration method in reinforcement learning; see [25]. The step 6 includes both policy evaluation and policy improvement.

B. Stability and Optimality Analysis

We will analyze the stability of the closed-loop system in the following theorem.

Theorem 2: The origin of the system (1) in closed-loop with (13) learned by data-driven control Algorithm 1 is an exponentially stable equilibrium.

Proof: For the vehicle i, the closed-loop system can be described in the following form

$$\dot{x}_i = (A_i - B_i K_{i,j^*})x_i + \sum_{k \in \mathcal{N}_i(t)} \frac{1}{|\mathcal{N}_i(t)|} B_i K_{i,j^*} x_k + D_i x_{i-1}$$

where, given a small enough constant ϵ_i, the matrix $A_i - B_i K_{i,j^*}$ is always a Hurwitz matrix.

For the leading vehicle, we can always find $\beta_1, \lambda_1 > 0$ such that

$$|x_1(t)| = |e^{(A_1 - B_1 K_{1,j^*})t} x_1(0)| \le \beta_1 e^{\lambda_1 t} |x_1(0)|$$

due to the fact that $x_0 \equiv 0$.

For the second vehicle, we can always find $\beta_2, \lambda_2 > 0$ such that

$$\begin{aligned}
|x_2(t)| &= |e^{(A_2 - B_2 K_{2,j^*})t} x_2(0)| + |B_2 K_{2,j^*} + D_2| \\
&\quad \times |\int_0^t e^{(A_2 - B_2 K_{2,j^*})(t-\tau)} x_1(\tau) d\tau| \\
&\le \beta_2 \, e^{\lambda_2 t} \left| \begin{bmatrix} x_1^T(0) & x_2^T(0) \end{bmatrix}^T \right|.
\end{aligned}$$

Similarly, we can observe that, for $i = 2, 3, \cdots, n$, there always exist $\beta_i > 0$, $\lambda_i > 0$ such that

$$|x_i(t)| \le \beta_i e^{\lambda_i t} \left| \begin{bmatrix} x_1^T(0) & x_2^T(0) & \cdots & x_i^T(0) \end{bmatrix}^T \right|$$

which directly implies that the closed-loop system is exponentially stable. The proof is completed. $\square$

The following theorem compares the minimum cost $J^* = x^T(0)P^*x(0)$ with the cost $J^\dagger$ associated with the distributed controller (13).

Theorem 3: There exists a constant $\mu > 0$ such that $J^\dagger \le \mu J^*$.

Proof: Write the closed-loop platooning system in a compact form

$$\dot{x} = A_c(t)x \tag{14}$$

where $x = \begin{bmatrix} x_1^T & x_2^T & \cdots & x_n^T \end{bmatrix}^T$.

The exponential stability of this system has been shown in Theorem 2. Therefore, the state transition matrix $\Phi(\tau, t)$ satisfies $|\Phi(\tau, t)| \le \beta e^{\lambda(\tau - t)}, \forall \tau \ge t \ge 0$. Let $P^\dagger(t) = \int_t^\infty \Phi^T(\tau, t)\Phi(\tau, t)d\tau$. It is checkable that there exists some $c_1, c_2 > 0$ such that $c_1|\phi|^2 \le \phi^T P^\dagger(t)\phi \le c_2|\phi|^2$, which implies that $P^\dagger(t)$ is positive definite and upper bounded by some $\sup_{t \ge 0}|P^\dagger(t)| < c_3$. The definition of $P^\dagger(t)$ shows that it is symmetric and continuously differentiable. By the fact that $\partial \Phi(\tau, t)/\partial t = -\Phi(\tau, t)A_c(t)$, $\Phi(\tau, \tau) = I$, and Leibniz integral rule, we have

$$\begin{aligned}
\dot{P}^\dagger(t) &= \int_t^\infty \frac{\partial}{\partial \tau} \left(\Phi^T(\tau, t)\Phi(\tau, t) \right) d\tau - \Phi^T(\tau, \tau)\Phi(\tau, \tau) \\
&= -P^\dagger(t)A_c(t) - A_c^T(t)P^\dagger(t) - I. \tag{15}
\end{aligned}$$

Along the solutions of (14), from (15), we have

$$\int_0^\infty |x^2|d\tau \le x^T(0)P^\dagger(0)x(0) \le c_2|x(0)|^2.$$
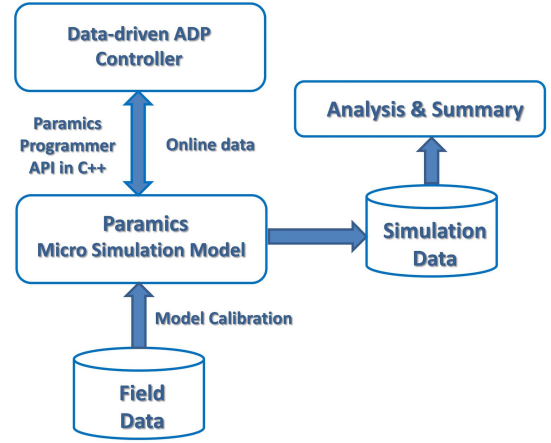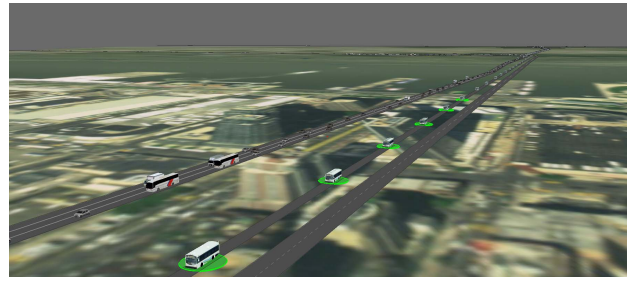

Fig. 4. Paramics simulation architecture.

Fig. 5. Snapshot of buses on XBL in closed-loop with data-driven CACC controller, simulation in Paramics.

Then, the cost $J^\dagger$ is bounded above by

$$\begin{aligned}
J^\dagger &\le \left[\lambda_M(Q) + n|R| \left(\max_i |K_{i,j^*}| \right)^2 \right] \int_0^\infty |x^2|d\tau \\
&\le \frac{c_2 \left[\lambda_M(Q) + n|R| \left(\max_i |K_{i,j^*}| \right)^2 \right]}{\lambda_m(P^*)} J^* \\
&:= \mu J^*. \tag{16}
\end{aligned}$$

The proof is thus completed. $\square$

IV. MICROSCOPIC TRAFFIC SIMULATION RESULT AND ANALYSIS

The proposed data-driven CACC Algorithm 1 is implemented in the micro-traffic simulation. Similar to reference [35], the data-driven controller is programmed via application programming interface (API) provided by Paramics. The API allows users to override the existing car following and other driver behavior characteristics [51]. There are four kinds of interfaces, named getting a value from (QPG), setting a value in (QPS), overriding (QPO), extended (QPX). When we finish the simulation, we collect simulation data to compare the control performance of the proposed data-driven control algorithm with that of the manual control. Fig. 4 shows how the control Algorithm 1 is implemented in Paramics simulation.

Note that the details of Paramics internal models are not exactly known by us. That is exactly why we use Paramics to validate the proposed data-driven idea. Fig. 5 is a snapshot
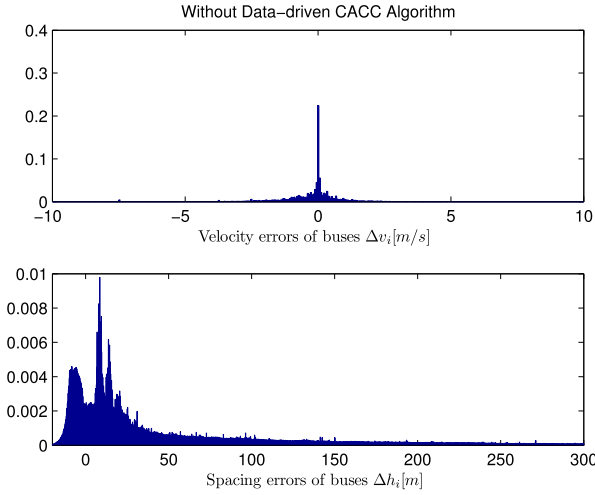
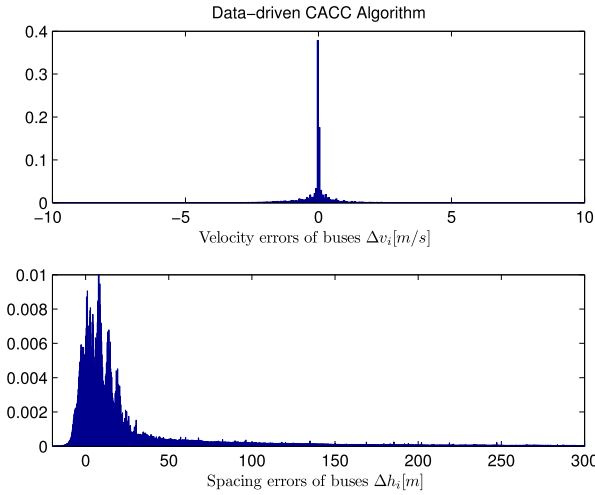Fig. 6. Histograms of velocity errors and spacing errors of buses without data-driven CACC control algorithm.

Fig. 7. Histograms of velocity errors and spacing errors of buses with data-driven CACC control algorithm.

Fig. 8. The comparison of learned value matrix P_{ij} and the optimal value matrix P_i^*.
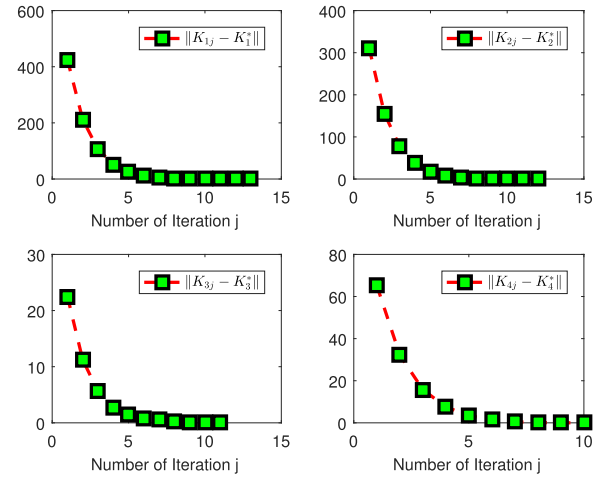
Fig. 9. The comparison of learned value matrix K_{ij} and the optimal value matrix K_i^*.

of buses on XBL (with green shape) by using data-driven control Algorithm 1. These buses operate with roughly the same headway.

Notice that Paramics uses its own micro-traffic model with a number of heuristic decision making rules for lane changing and exiting to mimic actual human decision making in practice. Hence, we let the default Paramics control method output the manual control performance. In order to minimize the stochasticity of the simulation model, five simulation runs are performed with different random seeds.

For the purpose of simulation, the online position, velocity, and acceleration data of buses are collected to learn the value matrix P_{ij} and control gain K_{ij} with the vehicle index i and the iteration j. In order to test the convergence of Algorithm 1, a platoon of 4 buses is taken as an example. The comparison of learned value matrix P_{ij} and corresponding optimal value matrix P_i^* (solving from ARE (6)) of the ith bus is depicted in Fig. 8, while the comparison of learned control gain K_{ij} and the optimal gain K_i^* is given in Fig. 9. It shows that the stopping criterion for all the subsystems is satisfied in less than 15 iterations.
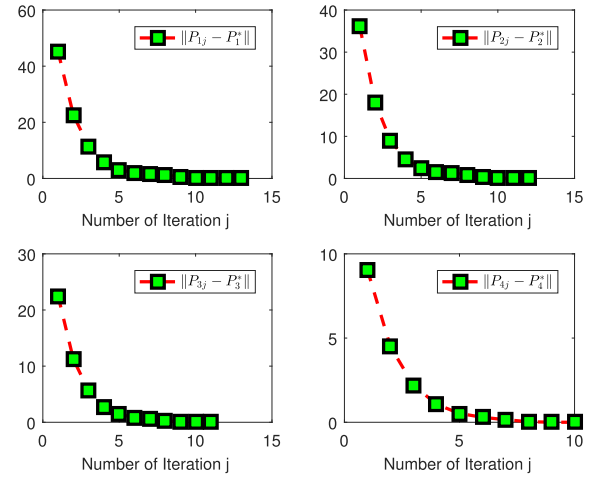
In this experiment, the communication range is set as $r_i = 300m$. The desired time headway is $\tau = 1.25s$. We test the effect of the platoon size on the travel time of autonomous buses. The result is illustrated in Tab. I with respect to different platoon size from $p = 3$ to $p = 7$. It is shown in the last row that the average travel time is ordered by $\bar{\mathcal{T}}_7 < \bar{\mathcal{T}}_4 < \bar{\mathcal{T}}_3 < \bar{\mathcal{T}}_5 < \bar{\mathcal{T}}_6$. It is suggested that the platoon size is set as $p = 4$ instead of a larger platoon size $p = 7$ since the former is able to reduce the computational load with only a slight increase of travel time, i.e., $\bar{\mathcal{T}}_4 - \bar{\mathcal{T}}_7 = 0.016min$.

Fig. 6 shows histograms of velocity and spacing errors of the buses on the XBL lane under manual control mode, while Fig. 7 shows histograms under data-driven CACC Algorithm 1. The velocity error distribution of both cases are bell-shaped. The spacing errors of both cases tend to generate distributions skewed to the left. The standard variations of velocity and headway errors under manual control mode are 1.8493 and 153.98, respectively. The standard variations of velocity and headway errors under CACC algorithm are 0.9799 and 127.23, both of which are smaller than that of manual control mode. The standard deviations of velocity and headway have been

TABLE I
TRAVEL TIMES $\mathcal{T}_p$ [MIN] UNDER DIFFERENT PLATOON SIZES p

Time Period	$\mathcal{T}_3$	$\mathcal{T}_4$	$\mathcal{T}_5$	$\mathcal{T}_6$	$\mathcal{T}_7$
6 : 15 − 6 : 30	8.9047	8.9047	8.9043	8.9043	8.9107
6 : 30 − 6 : 45	9.0507	8.9857	8.9887	8.9887	9.0013
6 : 45 − 7 : 00	9.1167	9.0907	9.1400	9.1400	9.0810
7 : 00 − 7 : 15	9.4367	9.5373	9.4943	9.5083	9.4953
7 : 15 − 7 : 30	10.1927	10.3640	10.4190	10.4473	10.3123
7 : 30 − 7 : 45	10.8710	10.7670	10.9080	11.0507	10.8750
7 : 45 − 8 : 00	11.1727	11.1957	11.2217	11.3757	11.1053
8 : 00 − 8 : 15	11.6953	11.6517	11.7110	12.0737	11.6443
8 : 15 − 8 : 30	11.6193	11.6627	11.7420	11.8133	11.7963
8 : 30 − 8 : 45	12.4987	12.4973	12.4570	12.6767	12.2467
8 : 45 − 9 : 00	13.0570	12.7650	12.9253	13.1873	12.5393
9 : 00 − 9 : 15	13.2240	13.2300	13.6047	13.5970	13.5183
9 : 15 − 9 : 30	13.8420	13.9233	14.0990	13.5940	13.9623
9 : 30 − 9 : 45	14.2677	13.9353	13.6137	13.9620	13.8010
9 : 45 − 10 : 00	12.4740	12.4783	12.3077	12.6440	12.4513
Average $\overline{\mathcal{T}}_p$	11.4282	11.3992	11.4358	11.5309	11.3827

TABLE II
COMPARISON OF AVERAGE TRAVEL TIMES UNDER DIFFERENT VOLUMES

Case	Average Travel Time [min]
Field	13.0073
Data-Driven CACC	11.3946
15% increase in Vol. Data-Driven CACC	12.2828
20% increase in Vol. Data-Driven CACC	12.5711
30% increase in Vol. Data-Driven CACC	13.0805

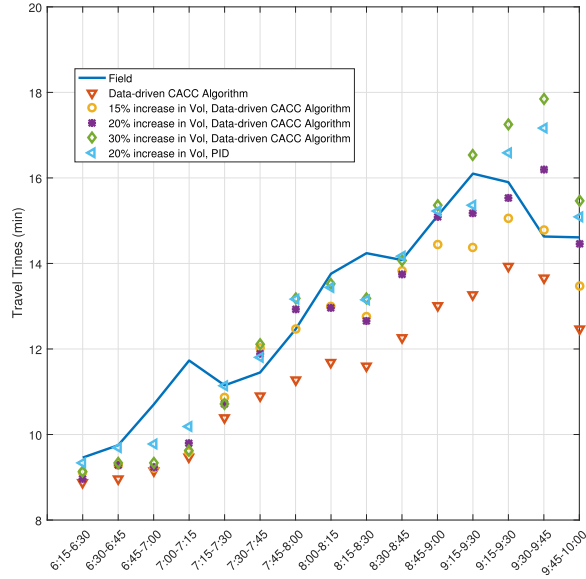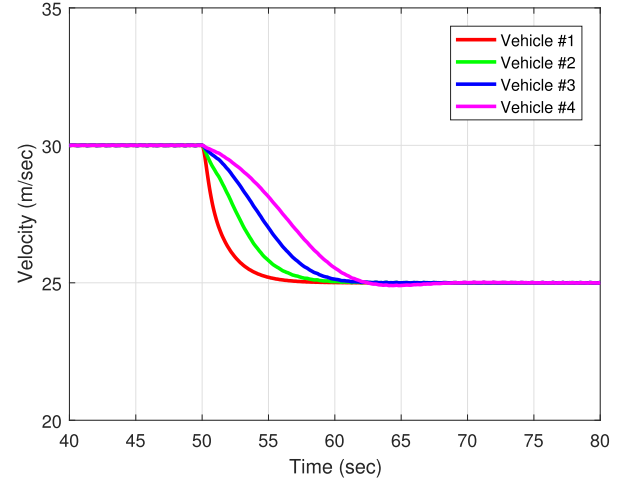Fig. 11. Velocities of the vehicular platoon.

Fig. 10. Travel time for different bus volumes.

used as surrogate safety measurements (SSM) to analyze the traffic safety; see [52] and references therein. Hence, it implies that the CACC is able to potentially reduce the crash risk.

We collect the travel times every 15 minutes using the proposed data-driven CACC algorithm through taking $p = 4$. For the purpose of comparison, we use the real XBL travel time data (field data) collected from the Lincoln Tunnel. It is depicted in Fig. 10 that the data-driven algorithm is able to save travel time for buses on the XBL. The volume of buses in the autonomous XBL is increased to observe the increase in travel time. It is checkable that the travel time is overall shorter than the present case (field) while the bus volume is increased by 30% from 6:15 AM to 9 AM. For the period 9-10 AM, since the current field bus volume is already at capacity, the proposed CACC algorithm does not produce as much benefit as before. During this hour, the travel time becomes close to the present case when the bus volume is increased by 20%. The maximum travel time when the bus

volume is increased by 20% (16.1933 minutes) is comparable with the maximum field travel time (16.0977 minutes) from 9 AM to 10 AM.

Tab. II illustrates the corresponding average travel time for different volumes of buses under the proposed approach. The average travel time of field data is 13.0073 minutes, which is close to that of the data-driven CACC algorithm with 30% increase in bus volume, i.e. 13.0805 minutes. For the purpose of comparison, we use PID control algorithm in [10]. It shows in Fig. 10 that the bus volume was increased by 20% under PID control. The proposed data-driven CACC method is able to further improve the traffic conditions for the whole corridor.

Last but not least, we select a platoon of four buses. Let the leader begin to decelerate from a steady-state velocity $30m/s$ to another steady-state $25m/s$ at $t = 50s$. Fig. 11 depicts the response of the whole platoon, showing that all the vehicles can smoothly track the new desired velocity without overshoot.

V. CONCLUSIONS

In this paper, a data-driven cooperative adaptive cruise control (CACC) method is proposed for controlling a fleet of autonomous buses on the exclusive bus lane of the Lincoln Tunnel corridor by means of reinforcement learning and optimal control theories. The proposed control method is able to increase the traffic throughput and save the travel time by reducing the impact of the human drivers and by removing the assumption on the exact knowledge of the vehicle dynamics.

The proposed data-driven method performs better than the PID control method used in [10] from both theoretical and

experimental perspectives. Theoretically, the proposed method can ensure the stability of the connected bus systems in the presence of unknown vehicle dynamics. Note that stability is a critically important factor in ensuring the safety of vehicles. Moreover, the proposed method yields an optimal controller with respect to a predefined cost. A key strategy of the proposed distributed controller scheme is the use of a vehicle-to-vehicle communication network such that each autonomous vehicle can communicate with multiple vehicles in the communication range. These observations show that the proposed method can improve transient performance for a closed-loop, connected bus system when compared with existing vehicle control methods. This contributes to smoother traffic flow and shorter travel times. The Paramics microscopic traffic simulation results show that, under the proposed control method, the travel times of buses in the autonomous exclusive bus lanes are close to the present day travel times when the bus demand is increased by 30%. Compared with the earlier PID method in [10], we further increase the traffic flow by 10%.

Future work includes developing advanced CACC methods for a connected bus system when nonlinear models are used, for mixed human-driven and autonomous vehicle environments, and for a vehicular network with changing topology. Future work also includes collecting more field data using automated image processing techniques and developing a novel application programming interface to improve the performance of the micro-simulation model.

REFERENCES

[1] The Port Authority of New York and New Jersey. *2016 Monthly Traffic and Percent of E-ZPass Usage*. Accessed: 18, 2016. https://www.panynj.gov/bridges-tunnels/pdf/traffic-e-zpass-usage-2016.pdf

[2] The Port Authority of New York and New Jersey. (2017). *The Lincoln Tunnel Exclusive Bus Lane*. [Online]. Available: https://www.panynj.gov/bridges-tunnels/lincoln-tunnel-xbl.html

[3] "Lincoln tunnel exclusive bus lane enhancement study," Port Authority NY NJ, New York, NY, USA, Tech. Rep., 2005.

[4] Parsons Brinckerhoff Consultants, "Trans-hudson commuting capacity study summary report," The Port Authority of New York and New Jersey, New York, NY, USA, Tech. Rep., 2016. [Online]. Available: https://www.panynj.gov/about/pdf/trans-hudson_commuting_capacity_study-summary_report_9-21-16.pdf

[5] "Lincoln tunnel hot lane feasibility study," Port Authority NY NJ, New York, NY, USA, Tech. Rep., 2009. [Online]. Available: https://www.panynj.gov/about/pdf/Lincoln-Tunnel-HOT-Lane-Feasibility-Study.pdf

[6] K. Ozbay, X. Ban, and D. Yang, "Developments in connected and automated vehicles," *J. Intell. Transp. Syst.*, vol. 22, no. 3, pp. 187–189, 2018.

[7] P. Kachroo, S. Agarwal, B. Piccoli, and K. Özbay, "Multiscale modeling and control architecture for V2X enabled traffic streams," *IEEE Trans. Veh. Technol.*, vol. 66, no. 6, pp. 4616–4626, Jun. 2017.

[8] P. Kachroo and K. Özbay, *Feedback Control Theory for Dynamic Traffic Assignment* (Advances in Industrial Control). Cham, Switzerland: Springer-Verlag, 2018.

[9] W. Gao, A. Odekunle, Y. Chen, and Z.-P. Jiang, "Predictive cruise control of connected and autonomous vehicles via reinforcementlearning," *IET Control Theory Appl.*, to be published. doi: 10.1049/iet-cta/2018/6031.

[10] K. Ozbay, T. Indrakanti, O. Yanmaz-Tuzel, and S. Iyer, "A microscopic simulation study of automated headway control of buses traveling on the exclusive bus lane on the Lincoln tunnel corridor—Final report," Dept. Civil Environ. Eng., Rutgers Univ., New Brunswick, NJ, USA, Tech. Rep., 2010. [Online]. Available: http://engineering.nyu.edu/citysmart/trbpaper/2010/TCC-FTA-Automated_Headway_Control_of_Bus_Final.pdf

[11] K. Ozbay, T. Indrakanti, O. Yanmaz-Tuzel, and S. Iyer, "A microscopic simulation study of automated headway control of buses traveling on the exclusive bus lane on the Lincoln tunnel corridor," in *Proc. 89th Annu. Meeting Compendium Papers DVD*, Washington, DC, USA, 2010, Paper 10-3495.

[12] J. I. Ge and G. Orosz, "Dynamics of connected vehicle systems with delayed acceleration feedback," *Transp. Res. C, Emerg. Technol.*, vol. 46, pp. 46–64, Sep. 2014.

[13] M. Wang, W. Daamen, S. P. Hoogendoorn, and B. van Arem, "Rolling horizon control framework for driver assistance systems. Part II: Cooperative sensing and cooperative control," *Transp. Res. C, Emerg. Technol.*, vol. 40, pp. 290–311, Mar. 2014.

[14] M. Wang, W. Daamen, S. P. Hoogendoorn, and B. van Arem, "Cooperative car-following control: Distributed algorithm and impact on moving jam features," *IEEE Trans. Intell. Transp. Syst.*, vol. 17, no. 5, pp. 1459–1471, May 2016.

[15] N. Chen, M. Wang, T. Alkim, and B. van Arem, "A robust longitudinal control strategy of platoons under model uncertainties and time delays," *J. Adv. Transp.*, vol. 2018, 2018, Art. no. 9852721.

[16] J. Ploeg, D. P. Shukla, N. van de Wouw, and H. Nijmeijer, "Controller synthesis for string stability of vehicle platoons," *IEEE Trans. Intell. Transp. Syst.*, vol. 15, no. 2, pp. 854–865, Apr. 2014.

[17] M. Wang, "Infrastructure assisted adaptive driving to stabilise heterogeneous vehicle strings," *Transp. Res. C, Emerg. Technol.*, vol. 91, pp. 276–295, Jun. 2018.

[18] M. Huang, W. Gao, and Z. P. Jiang, "Connected cruise control with delayed feedback and disturbance: An adaptive dynamic programming approach," *Int. J. Adapt. Control Signal Process.*, to be published, doi: 10.1002/acs.2834.

[19] J. V. Werf, S. Shladover, M. Miller, and N. Kourjanskaia, "Effects of adaptive cruise control systems on highway traffic flow capacity," *Transp. Res. Rec., J. Transp. Res. Board*, vol. 1800, pp. 78–84, Jan. 2002.

[20] B. van Arem, C. J. G. van Driel, and R. Visser, "The impact of cooperative adaptive cruise control on traffic-flow characteristics," *IEEE Trans. Intell. Transp. Syst.*, vol. 7, no. 4, pp. 429–436, Dec. 2006.

[21] S. Shladover, D. Su, and X.-Y. Lu, "Impacts of cooperative adaptive cruise control on freeway traffic flow," *Transp. Res. Rec., J. Transp. Res. Board*, vol. 2324, pp. 63–70, Dec. 2012.

[22] K. J. Malakorn and B. Park, "Assessment of mobility, energy, and environment impacts of IntelliDrive-based cooperative adaptive cruise control and intelligent traffic signal control," in *Proc. IEEE Int. Symp. Sustain. Syst. Technol.*, May 2010, pp. 1–6.

[23] V. Milanés, S. E. Shladover, J. Spring, C. Nowakowski, H. Kawazoe, and M. Nakamura, "Cooperative adaptive cruise control in real traffic situations," *IEEE Trans. Intell. Transp. Syst.*, vol. 15, no. 1, pp. 296–305, Feb. 2014.

[24] F. L. Lewis and D. Vrabie, "Reinforcement learning and adaptive dynamic programming for feedback control," *IEEE Circuits Syst. Mag.*, vol. 9, no. 3, pp. 32–50, Aug. 2009.

[25] R. S. Sutton and A. G. Barto, *Introduction to Reinforcement Learning*. Cambridge, MA, USA: MIT Press, 1998.

[26] Y. Zhu, D. Zhao, and X. Li, "Using reinforcement learning techniques to solve continuous-time non-linear optimal tracking problem without system dynamics," *IET Control Theory Appl.*, vol. 10, no. 12, pp. 1339–1347, 2016.

[27] D. Wang, D. Liu, H. Li, B. Luo, and H. Ma, "An approximate optimal control approach for robust stabilization of a class of discrete-time nonlinear systems with uncertainties," *IEEE Trans. Syst., Man, Cybern., Syst.*, vol. 46, no. 5, pp. 713–717, May 2016.

[28] W. Gao and Z.-P. Jiang, "Learning-based adaptive optimal tracking control of strict-feedback nonlinear systems," *IEEE Trans. Neural Netw. Learn. Syst.*, vol. 29, no. 6, pp. 2614–2624, Jun. 2018.

[29] V. Kyriakos, "Non-zero sum Nash Q-learning for unknown deterministic continuous-time linear systems," *Automatica*, vol. 61, no. 11, pp. 274–281, Nov. 2015.

[30] Z. Ni, H. He, and J. Wen, "Adaptive learning in tracking control based on the dual critic network design," *IEEE Trans. Neural Netw. Learn. Syst.*, vol. 24, no. 6, pp. 913–928, Jun. 2013.

[31] Y. Jiang, J. Fan, T. Chai, J. Li, and F. L. Lewis, "Data-driven flotation industrial process operational optimal control based on reinforcement learning," *IEEE Trans. Ind. Informat.*, vol. 14, no. 5, pp. 1974–1989, May 2018.

[32] Y. Jiang and Z.-P. Jiang, *Robust Adaptive Dynamic Programming*. Hoboken. NJ, USA: Wiley, 2017.

[33] W. B. Powell, *Approximate Dynamic Programming: Solving the Curses of Dimensionality*. New York, NY, USA: Wiley, 2007.

[34] D. P. Bertsekas and J. N. Tsitsiklis, *Neuro-Dynamic Programming*. Belmont, MA, USA: Athena Scientific, 1996.

[35] W. Gao, Z.-P. Jiang, and K. Ozbay, "Data-driven adaptive optimal control of connected vehicles," *IEEE Trans. Intell. Transp. Syst.*, vol. 18, no. 5, pp. 1122–1133, May 2017.

[36] W. Gao and Z.-P. Jiang, "Nonlinear and adaptive suboptimal control of connected vehicles: A global adaptive dynamic programming approach," *J. Intell. Robot. Syst.*, vol. 85, nos. 3–4, pp. 597–611, 2017.

[37] T. Yang, Z. Meng, D. V. Dimarogonas, and K. H. Johansson, "Global consensus for discrete-time multi-agent systems with input saturation constraints," *Automatica*, vol. 50, no. 2, pp. 499–506, 2014.

[38] V. D. Blondel, J. M. Hendrickx, and J. N. Tsitsiklis, "On Krause's multi-agent consensus model with state-dependent connectivity," *IEEE Trans. Autom. Control*, vol. 54, no. 11, pp. 2586–2597, Nov. 2009.

[39] "Regional traffic impact study for T100.321: Newark bay-hudson county extension (NBHCE), milepost N6.00 to N8.20 bridge deck reconstruction eastbound and seismic retrofit," MITS Lab. Rutgers RIME Lab., New York University Urban, New York, NY, USA, Tech. Rep., 2016. [Online]. Available: http://engineering.nyu.edu/citysmart/otherpaper/T100-321-Traffic_Impact_Analysis_Final.pdf

[40] (2017). *NJ Transit*. [Online]. Available: http://mybusnow.njtransit.com/bustime/home.jsp

[41] E. Morgul *et al.*, "Virtual sensors: Web-based real-time data collection methodology for transportation operation performance analysis," *Transp. Res. Rec., J. Transp. Res. Board*, vol. 2442, no. 1, pp. 106–116, 2014.

[42] A. Kurkcu and K. Ozbay, "Estimating pedestrian densities, wait times, and flows with Wi-Fi and Bluetooth sensors," *Transp. Res. Rec., J. Transp. Res. Board*, vol. 2644, pp. 72–82, 2017.

[43] S. Mudigonda and K. Ozbay, "Robust calibration of macroscopic traffic simulation models using stochastic collocation," *Transp. Res. C: Emerg. Technol.*, vol. 59, pp. 358–374, Oct. 2015.

[44] P. A. Ioannou and C. C. Chien, "Autonomous intelligent cruise control," *IEEE Trans. Veh. Technol.*, vol. 42, no. 4, pp. 657–672, Nov. 1993.

[45] P. Seiler, A. Pant, and K. Hedrick, "Disturbance propagation in vehicle strings," *IEEE Trans. Autom. Control*, vol. 49, no. 10, pp. 1835–1842, Oct. 2004.

[46] S. Li, K. Li, R. Rajamani, and J. Wang, "Model predictive multi-objective vehicular adaptive cruise control," *IEEE Trans. Control Syst. Technol.*, vol. 19, no. 3, pp. 556–566, May 2011.

[47] F. L. Lewis, D. Vrabie, and V. L. Syrmos, *Optimal Control*. Hoboken, NJ, USA: Wiley, 2012.

[48] W. Gao and Z.-P. Jiang, "Adaptive dynamic programming and adaptive optimal output regulation of linear systems," *IEEE Trans. Autom. Control*, vol. 61, no. 12, pp. 4164–4169, Dec. 2016.

[49] Y. Jiang and Z.-P. Jiang, "Computational adaptive optimal control for continuous-time linear systems with completely unknown dynamics," *Automatica*, vol. 48, no. 10, pp. 2699–2704, 2012.

[50] D. L. Kleinman, "On an iterative technique for Riccati equation computations," *IEEE Trans. Autom. Control*, vol. 13, no. 1, pp. 114–115, Feb. 1968.

[51] D.-H. Lee, P. Chandrasekar, and R.-L. Cheu, "Customized simulation modeling using PARAMICS application programmer interface," in *Proc. IEEE Intell. Transp. Syst. Conf.*, Aug. 2001, pp. 842–847.

[52] M. S. Rahman, M. Abdel-Aty, L. Wang, and J. Lee, "Understanding the highway safety benefits of different approaches of connected vehicles in reduced visibility conditions," *Transp. Res. Rec.*, vol. 2672, no. 19, pp. 91–101, 2018.

Jingqin Gao received the B.Sc. degree in science and technology of optical information from Tongji University, China, in 2010, and the M.Sc. degree in transportation planning and engineering from the New York University Tandon School of Engineering, USA, in 2012. She has been with the New York City Department of Transportation on Modeling and Data Analysis, New York University Tandon School of Engineering, to support the agency's internal planning, technical review processes, and coordinated with external agencies on regional projects, since 2012. She was involved in some of the key projects, including Manhattan Traffic Model, Off-Hour Deliveries, I-495 Managed Use Lane, Taxi GPS Analysis, Regional Traffic Impact Study for Newark Bay-Hudson County Extension Bridge Deck Reconstruction, and Research on Concrete Applications for Sustainable Transportation. Her research interests lie in offline and real-time simulation modeling, big data and machine learning approach for transportation, and transportation economics.

Kaan Ozbay joined the Center for Urban Science and Progress, Department of Civil and Urban Engineering, NYU, in 2013. He was a tenured Full Professor with the Department of Civil and Environmental Engineering, Rutgers University, until 2013. He is currently the Director of the C2SMART Tier-1 University Transportation Center, New York University Tandon School of Engineering. He has published approximately 300 refereed papers in scholarly journals and conference proceedings. He is an Editorial Board Member of the ITS journal. Since 1994, he has been the Principal Investigator or the Co-Principal Investigator of 80 projects supported at a level of more than \$11,000,000 by the National Science Foundation (NSF), NJDOT, NYMTC, NYSDOT, New Jersey Highway Authority, USDOT, FHWA, VDOT, CUNY University Transportation Research Center, Department of Homeland Security, and USDOT ITS Research Center of Excellence. He was the Founding Director of the Rutgers Intelligent Transportation Systems Laboratory. His research interests include the development of simulation models of large scale complex transportation systems, advanced technology and sensing applications for Intelligent transportation systems, the modeling and evaluation of traffic incident and emergency management systems, feedback-based online real-time traffic control techniques, traffic safety, the applications of operations research techniques in network optimization and humanitarian inventory control, and transportation economics. He was a recipient of the prestigious NSF CAREER Award.

Weinan Gao (M'18) received the B.Sc. degree and the M.Sc. degree in control theory and control engineering from Northeastern University, Shenyang, China, in 2011 and 2013, respectively, and the Ph.D. degree in electrical engineering from the New York University Tandon School of Engineering, in 2017. He is currently an Assistant Professor in electrical and computer engineering with the Allen E. Paulson College of Engineering and Computing, Georgia Southern University, Statesboro, GA, USA. His research interests include reinforcement learning, adaptive dynamic programming, optimal control, cooperative adaptive cruise control, intelligent transportation systems, sampled-data control systems, and output regulation theory. He was a recipient of the Best Paper Award from the IEEE International Conference on Real-time Computing and Robotics in 2018. He serves as an Associate Editor for *Neurocomputing* and an Editorial Board Member of *Neural Computing and Applications*.

Zhong-Ping Jiang (M'94–SM'02–F'08) received the B.Sc. degree in mathematics from the University of Wuhan, Wuhan, China, in 1988, the M.Sc. degree in statistics from the University of Paris XI, Paris, France, in 1989, and the Ph.D. degree in automatic control and mathematics from the École des Mines de Paris, Paris, in 1993. He is currently a Professor in electrical and computer engineering with the Department of Electrical and Computer Engineering, New York University Tandon School of Engineering, Brooklyn, NY, USA. He has authored or coauthored over 200 peer-reviewed journal papers, with a Google Scholar h-index of 73, and has also co-authored four books entitled *Stability and Stabilization of Nonlinear Systems* (Springer, 2011), *Nonlinear Control of Dynamic Networks* (Taylor & Francis, 2014), *Robust Adaptive Dynamic Programming* (Wiley-IEEE Press, 2017), and *Nonlinear Control Under Information Constraints* (Beijing: Science Press, 2018). His main research interests include stability theory, robust/adaptive/distributed nonlinear control, and adaptive dynamic programming and their applications to information, mechanical, and biological systems.

Prof. Jiang is a fellow of the International Federation of Automatic Control.